NOD1 sensing of house dust mite–derived microbiota promotes allergic experimental asthma

Saliha Ait Yahia, PhD,[a]* Camille Audousset, MD,[a]* Daniel Alvarez-Simon, PhD,[a]* Han Vorng, BSc,[a] Dieudonnée Togbe, PhD,[b] Philippe Marquillies, BSc,[a] Myriam Delacre, BSc,[a] Stéphanie Rose, BSc,[b] Hélène Bouscayrol, MD,[b] Aline Rifflet, PhD,[c,d,e] Valérie Quesniaux, PhD,[b] Ivo Gomperts Boneca, PhD,[c,d,e] Mathias Chamaillard, PhD,[a] and Anne Tsicopoulos, MD[a] *Lille, Orléans, and Paris, France*

Background: Asthma severity has been linked to exposure to gram-negative bacteria from the environment that are recognized by NOD1 receptor and are present in house dust mite (HDM) extracts. NOD1 polymorphism has been associated with asthma.

Objective: We sought to evaluate whether either host or HDM-derived microbiota may contribute to NOD1-dependent disease severity.

Methods: A model of HDM-induced experimental asthma was used and the effect of NOD1 deficiency was evaluated. Contribution of host microbiota was evaluated by fecal transplantation. Contribution of HDM-derived microbiota was assessed by 16S ribosomal RNA sequencing, mass spectrometry analysis, and peptidoglycan depletion of the extracts.

Results: In this model, loss of the bacterial sensor NOD1 and its adaptor RIPK2 improved asthma features. Such inhibitory effect was not related to dysbiosis caused by NOD1 deficiency, as shown by fecal transplantation of Nod1-deficient microbiota to wild-type germ-free mice. The 16S ribosomal RNA gene sequencing and mass spectrometry analysis of HDM allergen, revealed the presence of some muropeptides from gram-negative bacteria that belong to the Bartonellaceae family. While such HDM-associated muropeptides were found to activate NOD1 signaling in epithelial cells, peptidoglycan-depleted HDM had a decreased ability to instigate asthma *in vivo*.

Conclusions: These data show that NOD1-dependent sensing of HDM-associated gram-negative bacteria aggravates the severity of experimental asthma, suggesting that inhibiting the NOD1 signaling pathway may be a therapeutic approach to treating asthma. (J Allergy Clin Immunol 2021;■■■:■■■-■■■.)

Key words: *Asthma, allergy, house dust mite, T_H2 cells, NOD1, peptidoglycan, epithelial cells, microbiota*

An increasing body of evidence from clinical and experimental studies suggests that microbiota encompass a wide range of dynamic microbial communities that play a significant role in host immunity including protecting against asthma. Besides the putative effect of the respiratory microbiota in asthma,[1-3] intestinal dysbiosis appears to also play an important role.[4,5] Accordingly, host immune responses are T_H2-biased under germ-free (GF) conditions[6] and antibiotic-treated or GF animal models of allergen-induced asthma exhibit an exacerbated phenotype in either neonates[7,8] or adults.[9] However, much less attention has been paid to the microbiota derived from house dust mite (HDM), which is the most frequent cause of allergic asthma, although analysis of HDM extracts has revealed the presence of gram-negative bacteria that may likely arise from their intestines.[10,11] Although it is well established that viral infections are involved in 40% to 85% of asthma exacerbations,[12] a link has been established between adult asthma severity and exposure to indoor gram-negative bacteria.[13] Unique muropeptides from the peptidoglycan (PG) of such bacteria are sensed by the pattern recognition receptors NOD1[14,15] and NOD2, each receptor recognizing distinct PG structures. While NOD1 recognizes meso-diaminopimelic containing muramyl tripeptide, NOD2 recognizes muramyl dipeptide (MDP).[16] Both receptors signal via the downstream adaptor RIPK2, which then activates mitogen-activated protein kinase and the nuclear factor-κB (NF-κB) pathway. Of note, NOD1-mediated sensing of the gut microbiota participates in the development of lymphoid tissues, while its absence results in dysbiosis.[17] Additionally, genome-wide association studies have revealed a molecular link among polymorphisms of NOD1, asthma, and high levels of IgE.[18] In agreement, we have previously shown that a NOD1 agonist used as a systemic adjuvant exacerbates ovalbumin (OVA)-induced T_H2-mediated allergic asthma through dendritic cell activation,[19] and a recent article[20] has shown that RIPK2 promotes HDM-induced allergic airway inflammation by

From [a]the University of Lille, Centre National de la Recherche Scientifique (CNRS), Institut National de la Santé et de la Recherche Médicale, Centre Hospitalier Universitaire Lille, Institut Pasteur de Lille, U1019–Unite Mixte de Recherche (UMR) 9017–Centre d'Infection et d'Immunité de Lille, [b]the Laboratory of Experimental and Molecular Immunology and Neurogenetics, UMR 7355 CNRS—Universitaire of Orléans, France; [c]Institut Pasteur, Unité Biologie et Génétique de la Paroi Bactérienne; [d]the CNRS, UMR 2001; and [e]the Institut National de la Santé et de la Recherche Médicale, Équipe Avenir, Paris.

*These authors equally contributed to the work.

Supported by grants from Projets Transversaux de Recherche (18-16) from Institut Pasteur (to A.T., M.C., and I.G.B.), by Agence Nationale de Recherche 18-CE14-0020 (to A.T., M.C., and I.G.B.), and by CNRS of Orléans (France) and European funding in Region Centre-Val de Loire (Fonds Européens de Developpement Régional no. 2016-00110366 BIO-TARGET and EX005756 BIO-TARGET II). A.R. was supported by Investissement d'Avenir program, Laboratoire d'Excellence "Integrative Biology of Emerging Infectious Diseases" (ANR-10-LABX-62-IBEID).

Disclosure of potential conflict of interest: The authors declare that they have no relevant conflicts of interest.

Received for publication July 1, 2020; revised October 27, 2020; accepted for publication December 28, 2020.

Corresponding author: Anne Tsicopoulos, MD, Center for Infection and Immunity of Lille, U1019 Pulmonary Immunity, Institut Pasteur de Lille, 1 rue du Professeur Calmette, 59019 Lille Cedex, France. E-mail: anne.tsicopoulos@pasteur-lille.fr.

0091-6749/$36.00

https://doi.org/10.1016/j.jaci.2020.12.649

Abbreviations used
BAL: Bronchoalveolar lavage
FM: Fecal microbiota
GF: Germ-free
h: Human
HDM: House dust mite
HEK: Human embryonic kidney
IR: Index of reactivity
m: Mouse
MDP: Muramyl dipeptide
NF-κB: nuclear factor-κB
NHBE: Normal human bronchial epithelial
OVA: ovalbumin
PEPT: Peptide transporter
PG: Peptidoglycan
siRNA: Small, interfering RNA
WT: Wild type

favoring type 2 immunity. The aim of this study was to evaluate whether either host or HDM-derived microbiota may contribute to NOD1-dependent disease severity. Here we provide evidence that NOD1-dependent sensing of muropeptides from gram-negative bacteria present in HDM extracts exacerbate the severity of allergic airway inflammation, independently of the control by NOD1 of the composition of the gut microbiota from its host. These data identify a new mechanism of asthma aggravation linking HDM-derived microbiota and NOD1 and suggest that interfering with NOD1 signaling pathway may provide a therapeutic approach in this cumbersome disease, as well as for exacerbations of asthma driven by gram-negative bacteria.

METHODS

Reagents

Key reagents used are listed in Table E1 in this article's Online Repository (available at www.jacionline.org).

Mice

Wild-type (WT) female C57BL/6 mice (6 weeks of age) were purchased from Charles River (Wilmington, Mass). *Nod1*$^{-/-}$, *Nod2*$^{-/-}$, and *Ripk2*$^{-/-}$ mice were backcrossed on the C57BL/6 background at least 8 times. All animals were housed under specific pathogen-free conditions, in ventilated cages with absorbent bedding material, maintained on a 12-hour daylight cycle and with free access to commercial pelleted food and water *ad libitum*. GF mice were housed in flexible isolators. All animal experiments were approved by the regional ethical committee and authorized by the ministry of research and innovation (Autorisation de Projet utilisant des Animaux à des Fins Scientifiques no. 7874-2016070417344442 v3), and the animals' care was in accordance with institutional guidelines. For fecal transplantation, fresh fecal pellets from untreated WT or *Nod1*$^{-/-}$ female mice were resuspended in 1 mL of sterile PBS, and GF mice were reconstituted by oral gavage with 200 μL of the suspension. The remaining homogenate was kept frozen and analyzed for the status of fecal colonization.

HDM-induced allergic airway inflammation and treatment of extracts

HDM mice were sensitized intranasally with Dermatophagoides farinae extract kindly provided by Stallergenes/Greer (lot 9702026) at a high dose of 5 index of reactivity (5IR) (ie, 15 μg protein/40 μL of PBS) or a lower dose of 1IR (ie, 3 μg protein/40 μL) in order to have a strong and a moderate model of allergic inflammation, respectively. Control mice received 40 μL of PBS. Seven days after sensitization, mice where challenged intranasally with 40 μL of HDM or PBS daily for 5 consecutive days. Forty-eight hours later, mice were anesthetized, assessed for airway hyperresponsiveness, and sacrificed (Fig 1, *A*). For some experiments, HDM extracts were depleted in LPSs or in PG (see this article's Online Repository at www.jacionline.org). For all conditions, airway hyperresponsiveness and lung inflammation were assessed. Bronchoalveolar lavage (BAL) fluids were recovered. Lung samples were collected for protein extraction, RNA isolation, and histology analysis.

Airway responsiveness measurement

Mice were anesthetized with 0.5 mg/kg medetomidine (Domitor; Pfizer, Brooklyn, NY) and ketamine (Imalgene 1000; Merial, Duluth, Ga) and immediately intubated with an 18-gauge catheter, followed by mechanical ventilation using the FlexiVent (SCIREQ, Montreal, Quebec, Canada). Mice were exposed to nebulized PBS followed by increasing concentrations of nebulized methacholine (0-100 mg/mL) (Sigma-Aldrich, St Louis, Mo) using an ultrasonic nebulizer (Aeroneb; Aerogen, Mountain View, Calif). Return to baseline resistance was ensured prior to the administration of the next doses of methacholine. The mean value of measured resistances was calculated for each dose.

BAL analysis

A total volume of 1 mL of ice-cold PBS was used to gently wash the lungs. Cells from the lavage fluid were recovered by centrifugation at 135*g* for 5 minutes at 4°C. Cells were then resuspended in PBS and counted. Samples of this resuspended BAL were spun onto slides (Shandon Cytospin 4; Thermo Fisher Scientific, Waltham, Mass) and stained with May-Grünwald Giemsa (DiaPath, Martinengo, Italy) for differential cell count.

Serum collection and analysis

Blood was drawn from the abdominal vein. Serum was collected by centrifugation (5000*g* for 5 minutes) and stored at −20°C. Levels of total IgE and D farinae–specific IgG_1 were measured in collected sera by ELISA as indicated in the Online Repository.

Pulmonary histology

The left lobe of the lung from each mouse was fixed in Antigenfix (DiaPath) and embedded in paraffin (Histowax; HistoLab, Askim, Sweden) according to the manufacturer's indications. Lung sections of 5 μm were stained with a standard hematoxylin and eosin stain and periodic acid–Schiff staining kit (DiaPath) to evaluate the peribronchial inflammation and mucopolysaccharide staining for mucus, respectively.

Lung protein extracts

Lung lobe was homogenized in 1 mL of T-PER Tissue Protein Extraction Reagent (Thermo Fisher Scientific) buffer containing protease inhibitors (Roche Diagnostics, Rotkreuz, Switzerland). After 10 minutes on ice, the lysates were centrifuged at 13,000*g* for 5 minutes at 4°C and supernatants were collected for further cytokine and chemokine measurements. Total protein concentrations of lung extracts were measured using the Pierce BCA Protein Assay Kit (Thermo Fisher Scientific).

Human cell lines and primary human epithelial cells

Human embryonic kidney HEK293, human bronchial epithelium BEAS-2B, and human alveolar epithelial A549 cell lines, as well as normal human bronchial epithelial (NHBE) cells were cultured as indicated in the Online Repository.

HEK293 luciferase reporter cell assay

The luciferase NF-κB reporter assays, were performed by seeding HEK293 cells in 96-well plates at 5×10^4 cells per well and transfecting them with

expression plasmids producing either human (h) NOD1, mouse (m) Nod1, or mouse Nod2 (0.5 ng/well) in combination with the reporter plasmids pBxIV-luc (1 ng/well) and pEF-BOS-β-gal (25 ng/well) using Lipofectamine LTX with Plus Reagent (Invitrogen, Thermo Fisher Scientific) following manufacturer's recommendations. The reporter plasmids and the expression plasmids for hNOD1, hNOD2, mNod1, and mNod2 were kindly provided by Gabriel Nuñez and Naohiro Inohara (Ann Arbor, Mich). Details are provided in the Online Repository. The results were normalized by the expression of β-galactosidase to reflect the efficiency of transfection and expressed as fold expression of the plasmid-transfected cells.

Epithelial cell line stimulation and transfection with siRNA

BEAS-2B cells were stimulated with HDM at a final dose of 0.2 IR (ie, 6 μg protein/mL) unless otherwise stated in the figures, the synthetic NOD1 agonist FK565 (50 μg/mL; Fujisawa Pharmaceutical Company, Osaka, Japan) or MDP (10 μg/mL; InvivoGen, San Diego, Calif), after a 4-hour human recombinant IFN-β (20 ng/mL; PeproTech, Rocky Hill, NJ) priming. Culture supernatants and cell pellets were collected for cytokine quantification and RNA isolation. In some experiments, the stimuli were combined with a specific RIPK2 kinase inhibitor (AGV discovery) at a final concentration of 5 μmol/L. BEAS-2B cells were also stimulated with LPSs (InvivoGen) in combination with the RIPK2 inhibitor as a specificity control of the inhibitor. Except for mRNA analysis, HDM, FK565, and MDP stimulations were performed in presence of Lipofectamine LTX to enhance intracellular transport. Knockdowns of either *NOD1* or *NOD2* in BEAS-2B were obtained by a 48 hours small, interfering RNA (siRNA) transfection after a 4-hour human recombinant IFN-β (20 ng/mL; PeproTech) priming. NHBE cells were cultured as described in the Online Repository.

Generation of chimeric mice by bone marrow transplantation

Total body irradiated WT or *Nod1*$^{-/-}$ mice were transplanted with either WT or *Nod1*$^{-/-}$ bone marrow cells. Two months later, mice were sensitized and challenged with HDM as described above. Details are provided in the Methods of this article's Online Repository (available at www.jacionline.org).

Quantitative real-time PCR

Quantitative real-time PCR was performed using standard procedures described in the Online Repository. Primers used are listed in Table E2 in this article's Online Repository (available at www.jacionline.org).

ELISA measurement of cytokine chemokine

Murine cytokine (TSLP, IL-33) and chemokine (CCL17, CCL22) levels in lung protein extracts were assessed using commercial ELISA according to the instructions provided by the manufacturers (R&D Systems, Bio-Techne, Minneapolis, Minn; and e-Biosciences, Thermo Fisher Scientific). Human IL-6 and IL-8 (CXCL8) concentrations in BEAS-2B, A549 and NHBE cell culture supernatants were measured by ELISA using the ELISA Duoset kits (R&D Systems). The reasons of the choice of the different cytokines and chemokines are indicated in the Online Repository.

16S rRNA analysis

Fresh fecal samples were collected at the end of the experiment and immediately snap frozen in liquid nitrogen. Fecal DNA was isolated and sequenced at Genoscreen (https://www.genoscreen.fr). Quantification of bacterial diversity in HDM was assessed by 16S rRNA sequencing on the V3/V4 region. Details are provided in the Online Repository.

LC-MS/MS method

HDM extracts were analyzed by LC-MS/MS method as described in the Online Repository.

Statistical analysis

For bacterial taxonomy analysis, we used the microbiome analyst software to determine community properties. Principal coordinates analysis plots using unweighted unique fraction metric distances were used to analyze the segregation between WT fecal microbiota (FM)→GF and Nod1$^{-/-}$FM→GF mice using analysis of group similarities statistical analysis. Alpha diversity, calculated as the Channon index, was analyzed using Mann-Whitney *U* test. *P* values <.05 were considered to be statistically significant. For animal and cell analyses, data were analyzed using Prism 8.0 (GraphPad Software, San Diego, Calif). For normally distributed data, significance of differences between groups was evaluated by 1-way ANOVA with Bonferroni *post hoc* test for multiple comparisons. For pairwise comparisons the 2-tailed Student *t*-test was used. For airway resistance, the 2-way analysis of variance test was used. Nonnormally distributed data were analyzed using the Kruskal-Wallis *H* with Dunn *post hoc* test. For i*n vitro* cell experiments, 3 to 4 biological replicates were performed, and the experiment was repeated 2 to 3 times. For *in vivo* experiments, the number of mice per group is indicated in the figure legends. *P* values <.05 were considered to be statistically significant.

RESULTS

Nod1 signaling aggravates HDM-induced allergic airway disease through Ripk2

The *in vivo* effect of Nod1 signaling was investigated in a model of 5IR (ie, 15 μg protein/mL) HDM-induced asthma[21] (Fig 1, *A*) in C57BL6/J mice deficient or not in *Nod1*. HDM-challenged WT mice exhibited all the cardinal features of allergic airway inflammation, including increase in total cell, eosinophil, neutrophil, and macrophage numbers in BAL (Fig 1, *B*), total IgE, and HDM-specific IgG_1 antibodies (Fig 1, *C*), and levels of lung T_H2/T_H17 cytokines and some pro-T_H2 chemokines (Fig 1, *D*; see Fig E1, *A*, in this article's Online Repository at www.jacionline.org). All these features were strongly diminished in *Nod1*$^{-/-}$ mice, except for the humoral response and T_H17-type cytokine levels (Figs 1, *B-D*, and E1, *A*). Lung sections from HDM-challenged mice showed that the increases in periodic acid–Schiff –stained mucus and in hematoxylin and eosin–stained cellular infiltrates in WT mice were decreased in the absence of Nod1 (Figs 1, *E*, and E1, *B*, respectively). Functionally, airway resistance in response to methacholine challenge was totally inhibited in HDM-challenged *Nod1*$^{-/-}$ versus WT mice (Fig 1, *F*). Likewise, *Nod2* deficiency led to a decrease in BAL cell recruitment after HDM challenge (Fig 1, *G*) and not in the humoral response (Fig 1, *H*). By contrast, there was no statistically significant decrease in T_H2 and pro-T_H2 lung cytokines and chemokines except for CCL2 and keratinocyte-derived chemokine (Figs 1, *I*, and E1, *C*), and no decrease in airway resistance (Fig 1, *J*). Given that Nod1 and Nod2 signal via the downstream adaptor Ripk2, we next evaluated whether a similar pattern of response was observed in *Ripk2*$^{-/-}$ mice. Miller *et al*[20] have recently reported that HDM-induced allergic airway inflammation is reduced in *Ripk2*$^{-/-}$ mice in a model similar to our 5IR model. Therefore, we assessed *Ripk2*$^{-/-}$ mice in a 1IR (3 μg protein/mL) model of HDM-induced allergic inflammation. There was a total inhibition of BAL cell recruitment, in particular of eosinophils (Fig 2, *A*), no changes in the humoral response (Fig 2, *B*), a decrease of T_H2-type cytokines and chemokines (Fig 2, *C*), of mucus production (Fig 2, *D*) and of airway resistance (Fig 2, *E*). In contrast to the Miller *et al*[20] article, it is of note that we did not observe changes in the humoral response, but we additionally observed abolition of a cardinal feature of

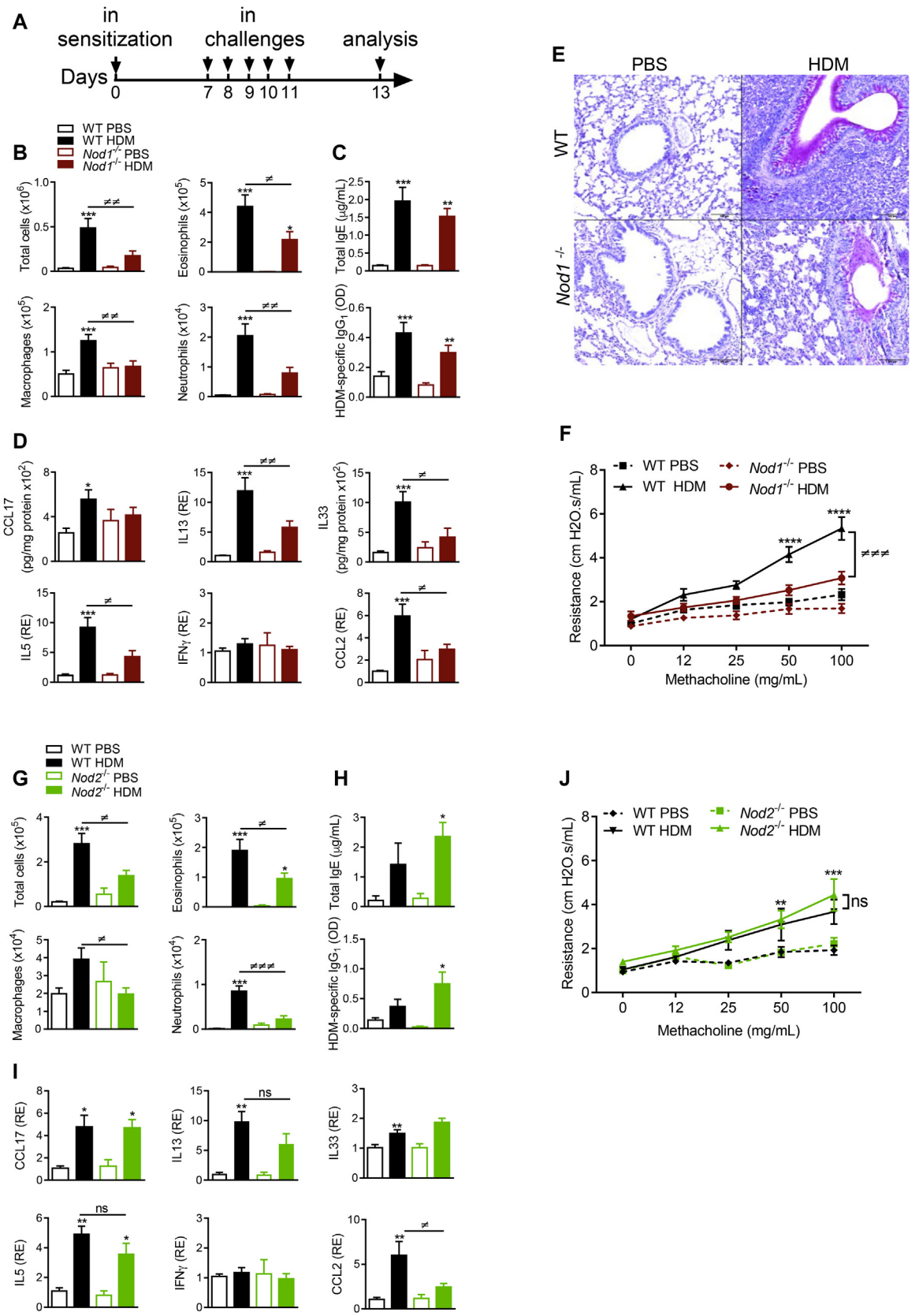

FIG 1. Nod1 signaling aggravates HDM-induced allergic airway disease. **A,** Protocol of HDM-induced experimental asthma. **B,** BAL cell counts in WT and *Nod1*$^{-/-}$ mice challenged with PBS or HDM. **C,** ELISA detection of T_H2 humoral response in WT and *Nod1*$^{-/-}$ mice challenged with PBS or HDM. **D,** Protein and mRNA relative expression (*RE*) of cytokines and chemokines assessed by ELISA and quantitative real-time -PCR in

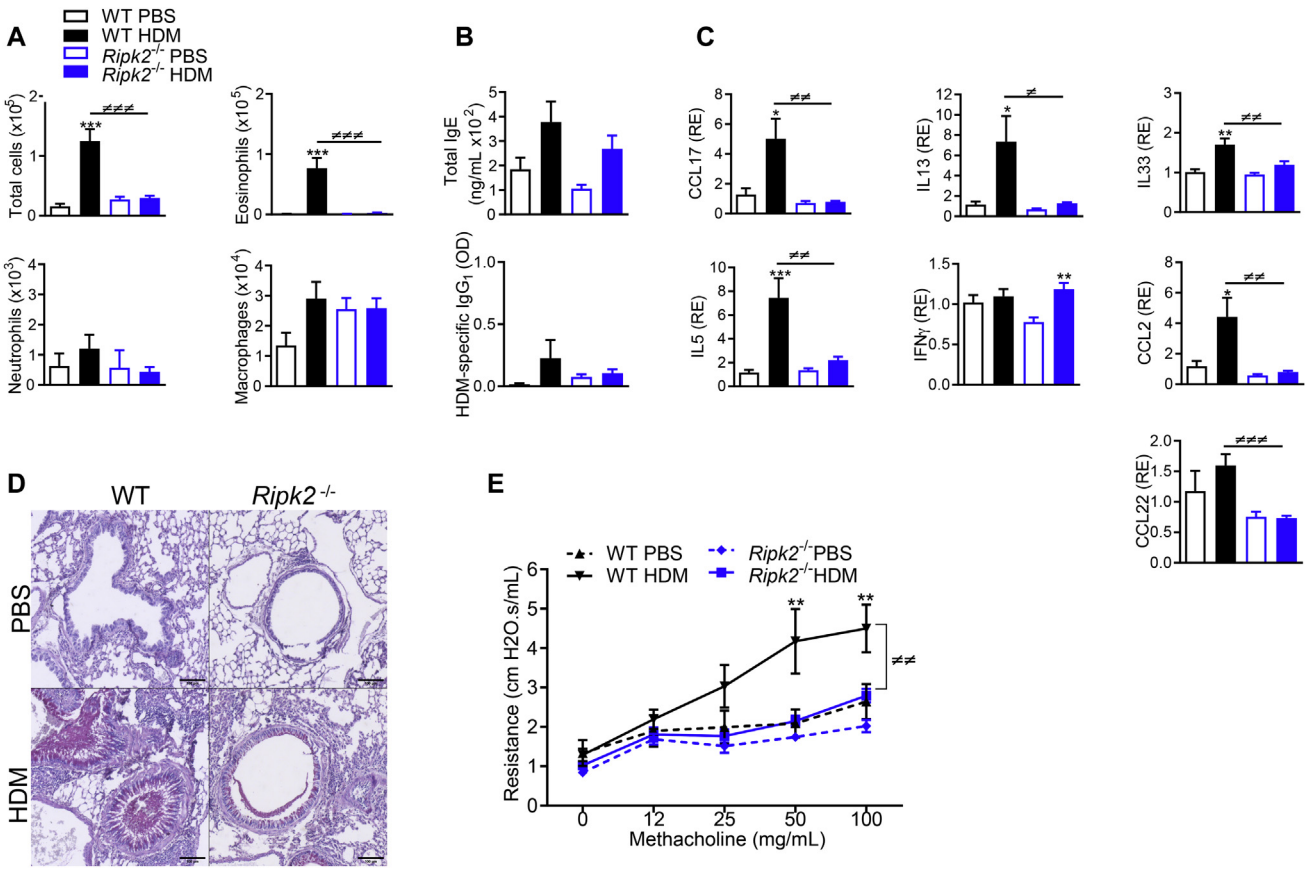

FIG 2. Nod1 signaling aggravates HDM-induced allergic airway disease through Ripk2. **A,** BAL cell counts in WT and *Ripk2*$^{-/-}$ mice challenged with PBS or low dose of HDM. **B,** ELISA detection of total IgE and HDM-specific IgG_1 antibody in WT and *Ripk2*$^{-/-}$ mice challenged with PBS or low dose of HDM. **C,** Protein and mRNA RE of cytokines and chemokines assessed by ELISA and quantitative real-time PCR in lung extracts from WT and *Ripk2*$^{-/-}$ mice challenged with PBS or low dose of HDM. **D,** Representative microphotographs of periodic acid–Schiff–stained lung sections in WT and *Ripk2*$^{-/-}$ mice. Bars = 100 μm. **E,** Airway resistances of WT and *Ripk2*$^{-/-}$ mice challenged with PBS or low dose of HDM. Data are presented as mean ± SEM of n = 6 to 12 for Ripk2. *$P < .05$, **$P < .01$, ***$P < .001$ versus PBS; $^{\neq}P < .05$, $^{\neq\neq}P < .01$, $^{\neq\neq\neq}P < .001$ one-way ANOVA for all except airway resistance, which is 2-way ANOVA.

asthma, that is, airway resistance in *Ripk2*$^{-/-}$ and *Nod1*$^{-/-}$ but not *Nod2*$^{-/-}$ mice. Taken together, these data demonstrate that Nod1, but not Nod2 signaling, is involved in the severity of HDM-induced airway disease through Ripk2 activation.

Dysbiotic gut microbiota caused by Nod1 deficiency does not impact HDM-induced allergic airway disease risk

Because *Nod1*$^{-/-}$ mice harbor a dysbiotic gut flora, we next assessed whether such dysbiosis may influence the development of experimental asthma. Transplantation of fresh fecal homogenates from WT or *Nod1*$^{-/-}$ donor mice was performed in control GF recipients (referred to as WT or *Nod1*$^{-/-}$ FM→GF, respectively). Five weeks later, recolonized mice were subjected to the HDM protocol (Fig 3, *A*). Both groups of mice challenged with HDM, compared with the PBS groups, exhibited similar increased BAL cell recruitment (Fig 3, *B*), humoral response (Fig 3, *C*), T_H2-type response (Fig 3, *D*), and airway resistance (Fig 3, *E*). To evaluate the gut bacterial ecosystem of recolonized mice, fecal pellets were collected at the end of the experiments and analyzed by 16S rRNA phylogenetic profiling. Principal coordinates analysis plots using unweighted unique

lung extracts from WT and *Nod1*$^{-/-}$ mice challenged with PBS or HDM. **E,** Representative microphotographs of periodic acid–Schiff–stained lung sections in WT and *Nod1*$^{-/-}$ mice. Bars = 100 μm. **F,** Airway resistance of WT and *Nod1*$^{-/-}$ mice challenged with PBS or HDM. **G,** BAL cell counts in WT and *Nod2*$^{-/-}$ mice challenged with PBS or HDM. **H,** ELISA detection of T_H2 humoral response in WT and *Nod2*$^{-/-}$ mice challenged with PBS or HDM. **I,** Protein and mRNA RE of cytokines and chemokines assessed by ELISA and quantitative real-time PCR in lung extracts from WT and *Nod2*$^{-/-}$ mice challenged with PBS or HDM. **J,** Airway resistance of WT and *Nod2*$^{-/-}$ mice challenged with PBS or HDM. Data are presented as mean ± SEM of n = 12 to 22 animals per group for Nod1 and n = 5 to 9 animals per group for Nod2 experiments. *$P < .05$, **$P < .01$, ***$P < .001$ versus PBS, ****$P < .0001$; $^{\neq}P < .05$, $^{\neq\neq}P < .01$, $\neq\neq\neq P < .001$, 1-way ANOVA for all except airway resistance, which is 2-way ANOVA. *NS*, Not significant.

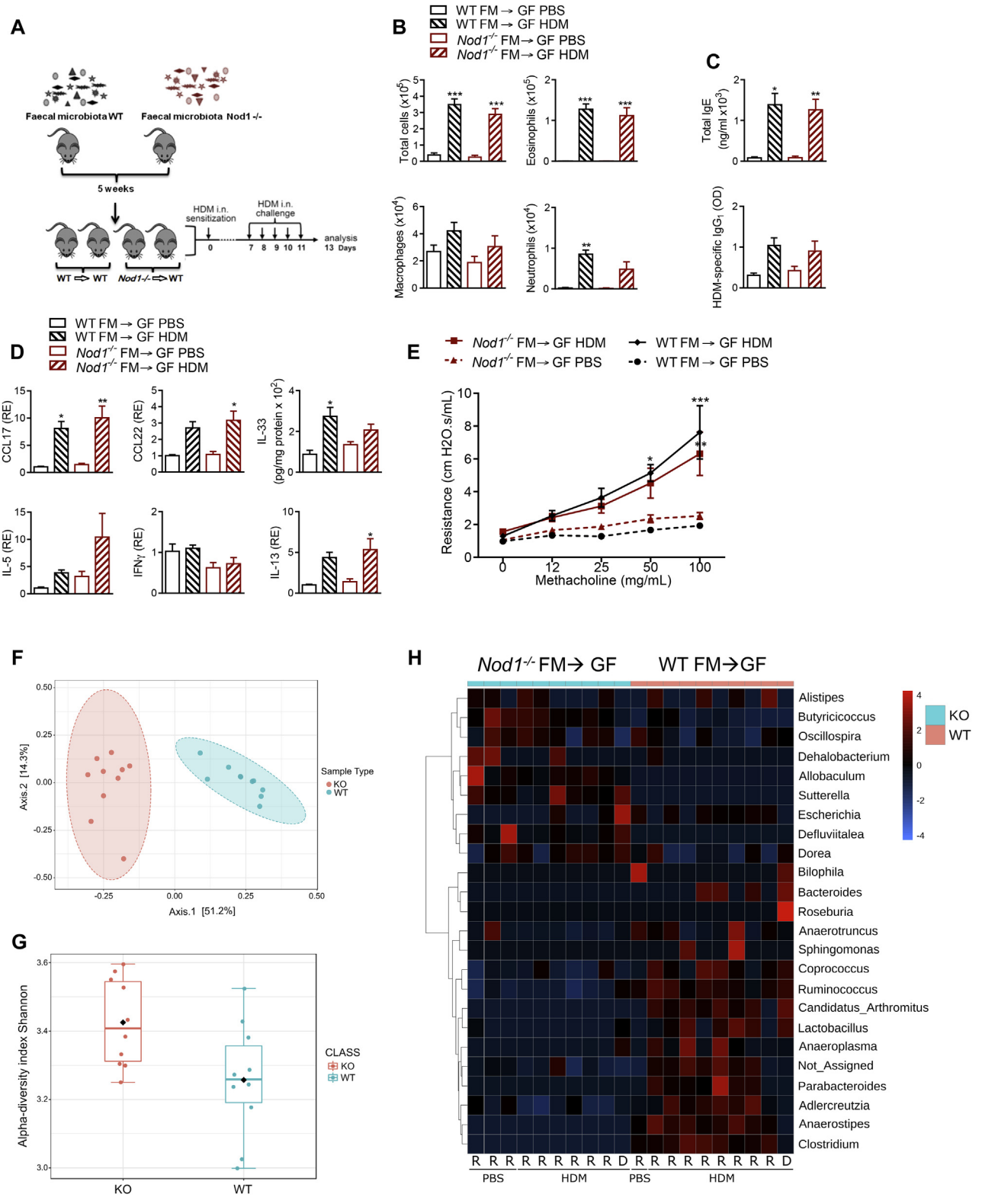

FIG 3. Dysbiotic gut microbiota caused by Nod1 deficiency does not impact HDM-induced allergic airway disease risk. **A,** Protocol of fecal transplantation. **B,** BAL cell counts in WT and *Nod1*$^{-/-}$ FM → GF mice challenged with PBS or HDM. **C,** ELISA detection of T_H2 humoral response in WT and *Nod1*$^{-/-}$ FM → GF mice challenged with PBS or HDM. **D,** Protein and mRNA RE of cytokines and chemokines assessed by ELISA and quantitative real-time PCR in lung extracts from WT and *Nod1*$^{-/-}$ FM → GF mice challenged with PBS or HDM. **E,** Airway resistance of WT and *Nod1*$^{-/-}$ FM → GF mice challenged with PBS or HDM. Data are presented as mean ± SEM of n = 4 to 7 animals per group. Data are representative of 2 independent experiments. **P* < .05 ***P* < .01 versus PBS. One-way ANOVA for all except airway resistance, which is 2-way ANOVA. **F,** Principal coordinates analysis plots using unweighted unique fraction metric distances of feces from WT FM → GF (*WT*) and *Nod1*$^{-/-}$ FM → GF mice (*KO*). $P \leq .001$ between the 2 groups, analysis of group similarities. **G,** Alpha diversity assessed by the Shannon index of feces from WT and *Nod1*$^{-/-}$ KO mice. $P \leq .01$ between the 2 groups, Mann-Whitney *U* test. **H,** Heat map of the top most abundant genera of feces from receivers (*R*) of WT, *Nod1*$^{-/-}$ KO mice challenged with PBS or HDM, and from initial donors (*D*). *in*, Intranasal.

fraction metric distances highlighted the segregation between ex-GF mice ($P \leq 001$, analysis of group similarities statistical analysis) (Fig 3, *F*). Alpha diversity, calculated as the Shannon index, showed significant differences between the groups of ex-GF mice ($P \leq 01$, Mann-Whitney U test) (Fig 3, *G*). Heat map of the top-most abundant genera illustrates the major differences in the composition of both groups of mice and the similarities with the microbiota composition from donors' feces (Fig 3, *H*). No difference was observed between PBS- and HDM-treated mice whatever the genotype of the donor mice. Altogether these data underline that the compositional changes in the gut microbiota of *Nod1*$^{-/-}$ mice were not responsible for their protection against HDM-induced disease.

HDM-associated muropeptides are sensed by NOD1 in epithelial cells via RIPK2

Quantification of bacterial diversity in HDM extracts by 16S rRNA sequencing revealed that 87.7% of the assembled reads associated with members of the gram-negative Bartonellaceae family (Fig 4, *A*). To identify specific PG moieties, HDM extracts were analyzed by MS through a targeted approach specifically looking at well-characterized muropeptides. Both DAP-containingmuramyl tripeptide and MDP, sensed by NOD1 and NOD2, respectively, were detected and their presence confirmed by fragmentation (Fig 4, *B* and *C*, and see Table E3 in this article's Online Repository at www.jacionline.org). Next, the effect of HDM was evaluated on human embryonic kidney 293 (HEK293) cells harboring a NF-κB–dependent luciferase reporter and expressing *hNOD1*, *mNod1*, or *mNod2* and normalized for transfection efficiency using a β-galactosidase control vector. All positive controls induced NF-κB activation (Fig 4, *D*). HDM extracts elicited a dose-dependent increase in both hNOD1- and mNod1-dependent luciferase activity, but only an effect at the highest dose of 4IR (ie, 60 μg protein/mL) for mNod2 activity (Fig 4, *D*). As the allergen first encounters epithelial cells, human bronchial epithelial BEAS-2B cells were primed with IFN-β[22] to increase the baseline expression of *NOD1*. The role of Nod1 signaling pathway was subsequently assessed by quantifying their cytokine production in response to HDM. HDM stimulation elicited a dose-dependent increase in the production of IL-6 and IL-8 by BEAS-2B cells with an effect starting at 0.2IR (6 μg protein/mL) and maximal at 4IR (120 μg protein/mL) (Fig E2, *A*, in this article's Online Repository at www.jacionline.org). BEAS-2B stimulation by HDM induced a clear increase in *NOD1* and *NOD2* mRNA (Fig 4, *E*). Although IFN-β increased *NOD1/2* expression and FK565-induced cytokine production (Fig E2, *B*), no effect was noticed on the response to HDM (Fig E2, *C*). As expected, the addition of a specific RIPK2 inhibitor belonging to the 4-amino-quinolines inhibited both IL-6 and IL-8 increases in response to FK565 positive control (Fig 4, *F*), but did not modulate the response to LPSs (Fig E2, *D*). HDM stimulation induced a stronger production of IL-6 and IL-8 (Fig 4, *F*) with a partial inhibitory noncytotoxic effect (Fig E2, *E*) of RIPK2 antagonist (Fig 4, *F*). The same results were observed for the human alveolar epithelial cell A549 (Fig E2, *F*). The respective roles of NOD1 and NOD2 were next assessed by transfecting BEAS-2B cells with specific siRNA. As compared to control and *NOD2* siRNAs, *NOD1* siRNA strongly inhibited FK565- and HDM-induced IL-6 and IL-8 production (Figs 4, *G*, and E2, *G*). Similar observation was noticed on HDM-induced IL-33 mRNA expression (Fig E2, *H*). Results were further confirmed using NHBE cells. Stimulation with HDM elicited a dose-dependent increase in IL-8 production as well as in *NOD1/2* mRNA expression in primary epithelial cells (Fig 4, *H*). Treatment with the RIPK2 antagonist strongly inhibited HDM-induced IL-8 production (Fig 4, *H*). The lack of effect of NOD2 led us to evaluate the mRNA expression of *PGLYRP2*, an enzyme that displays amidase activity known to degrade some NOD2-activating muropeptides. HDM stimulation was able to induce this enzyme both *in vitro* in BEAS-2B cells as well as *in vivo* in the lungs of HDM-challenged mice (Fig 4, *I*). In contrast, we failed to detect any change in the expression of PGLYRP1, another member of the peptidoglycan recognition protein family that was shown to be involved in HDM-induced allergic airway inflammation in the allergy-prone BALB/c mice[23-25] (Fig E2, *I*). Furthermore, the transporter peptide transporter (PEPT) 2, allowing uptake of NOD1 ligands, was highly expressed in both BEAS-2B cells and in the lungs of HDM-challenged mice as compared with PEPT1 transporter, which specialized in the transport of NOD2 ligand MDP (Fig 4, *J*). These data show that HDM triggers cytokine production by epithelial cells through a NOD1-dependent pathway involving RIPK2 signaling.

Nod1 expressed by radio-resistant cells mediate HDM-induced allergic airway inflammation

To evaluate the specific contribution of nonhematopoietic structural cells, in particular epithelial cells, versus the role of hematopoietic cells on Nod1-dependent HDM-induced airway inflammation, chimeric mice were generated expressing either Nod1$^{-/-}$ hematopoietic cells and structural WT cells (Nod1$^{-/-}$ → WT) or Nod1$^{-/-}$ structural cells together with WT hematopoietic cells (WT → Nod1$^{-/-}$). WT → WT and Nod1$^{-/-}$ → Nod1$^{-/-}$ groups served as controls. Analysis of BAL showed that the total cell, as well as eosinophil and neutrophil numbers, were increased after HDM challenge in the Nod1$^{-/-}$ → WT and the WT → WT mice, whereas they were diminished in the WT → Nod1$^{-/-}$ and Nod1$^{-/-}$ → Nod1$^{-/-}$ mice (Fig 5, *A*). The humoral response was not significantly modified after HDM challenge, whatever the group (Fig 5, *B*). While most tested cytokines were increased after HDM challenge in the WT → WT and Nod1$^{-/-}$ → WT mice, these were either decreased or abolished in WT → Nod1$^{-/-}$ and Nod1$^{-/-}$ → Nod1$^{-/-}$ mice (Fig 5, *C*). In agreement with our *in vitro* data, chimera experiments demonstrated that Nod1 expressed by structural cells mediates HDM-induced airway inflammation. However, CCL2, IL-13, and IL-33 were significantly decreased after HDM challenge in the Nod1$^{-/-}$ → WT group compared with in the WT → WT mice (Fig 5, *C*). This suggests that such induction of CCL2, IL-13, and IL-33 by HDM in WT mice reconstituted with Nod1-expressing hematopoietic cells is not sufficient for exacerbating HDM-induced airway inflammation.

Severity of allergic airway disease is decreased in response to PG-depleted but not LPS-depleted HDM

Among bacterial moieties, LPSs have been described to either favor or inhibit OVA-induced experimental asthma, according to their abundance.[26] To evaluate whether LPSs present in HDM were playing a role in the observed results, we

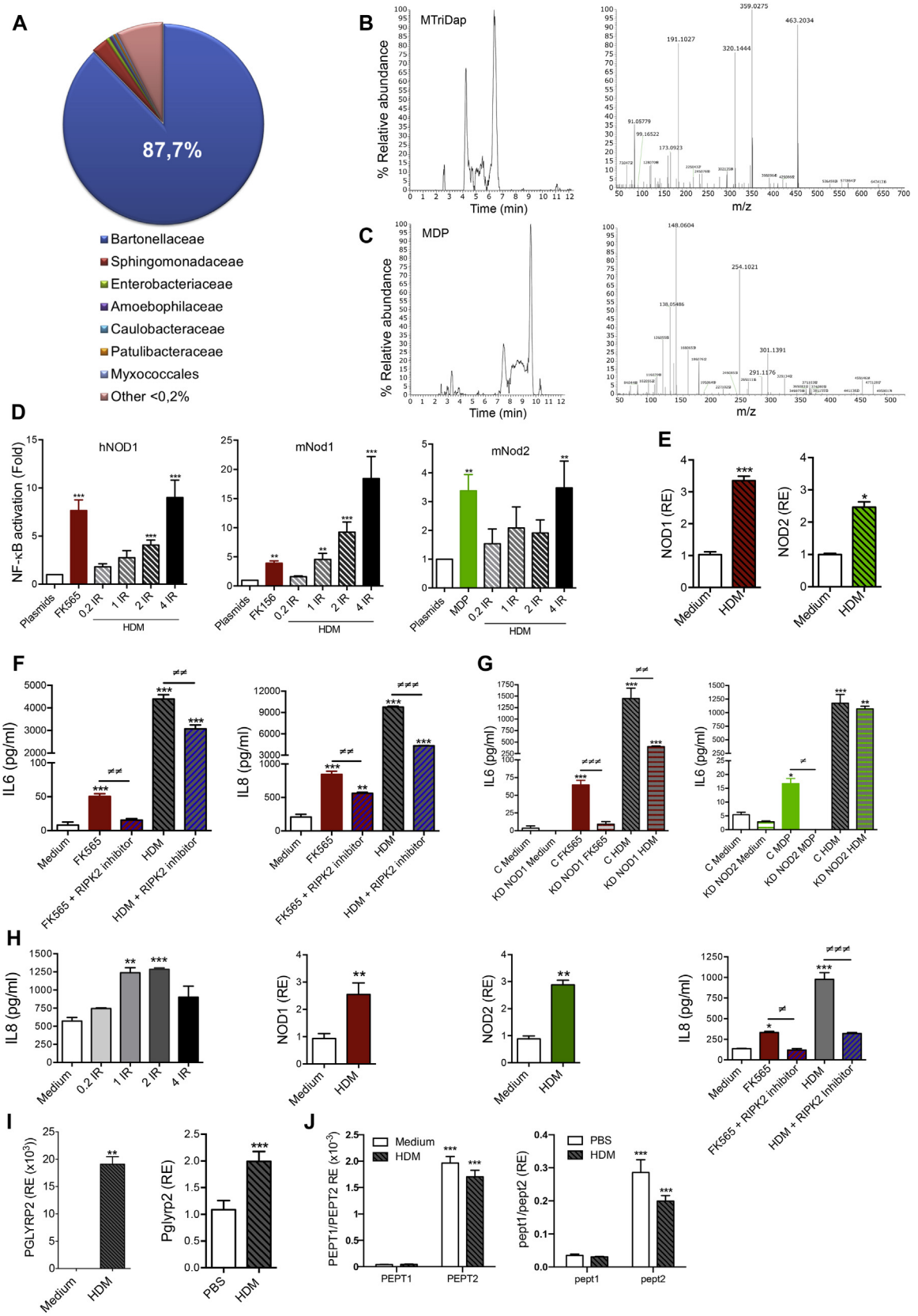

FIG 4. HDM-associated muropeptides are sensed by NOD1 in epithelial cells via RIPK2. **A,** High throughput sequencing analysis of HDM. **B,** Extract ion chromatograms of HDM corresponding to the protonated DAP-containing muramyl tripeptide (MTriDap) (m/z 666.2843) and its MS/MS fragmentation with a normalized collision energy equal to 25% in the high energy collision dissociation cell of QExactive Focus. The specific fragments are recorded in Table E3. **C,** Extract ion chromatograms of HDM corresponding to the protonated

depleted LPSs by purification on a resin column. *In vitro,* in NF-κB reporter cells, LPS-low HDM was still able to dose-dependently activate Nod1 (Fig E3, *A*, in this article's Online Repository at www.jacionline.org). As the concentration of LPSs was not biologically relevant for exacerbating the immunopathology in response to 1IR (2 ng/IR) we only used the 5IR HDM-induced protocol. *In vivo*, LPS-low HDM challenges led to an increase in most of the parameters of experimental asthma including BAL total cell recruitment, T_H2-type cytokine expression and airway hyperreactivity (Fig E3, *B, D,* and *E*) similar to that observed with native HDM challenges. The only parameter that was not induced by LPS-low HDM was the humoral response, which remained at basal levels (Fig E3, *C*). To evaluate the role of PG in NOD1-dependent effect, HDM extracts were digested with mutanolysin and proteins precipitated by organic solvents, and the corresponding pellets and supernatants were assessed on mNod1 activity. Presence or absence of PG was confirmed by MS in the supernatants and pellets, respectively (Fig 6, *A*). The PG-free pellets did not exhibit dose-dependent activation of mNod1 reporter activity, whereas the PG-containing supernatants activated the luciferase activity with significant effects at 4IR to 6IR (ie, 60 μg to 90 μg protein/mL) of initial HDM input (Fig 6, *B*). Next, the effect of PG depletion after normalization for final allergen content was evaluated in both HDM models to ascertain the results. In the 5IR HDM model, PG-depleted HDM challenges led to a reduction in BAL total cell recruitment, including mainly eosinophils (Fig 6, *C*), and no changes in the humoral response (Fig 6, *D*), but they did lead to a strong decrease in T_H2-type cytokines and an increase in IFN-γ (Fig 6, *E*). Airway resistance was also reduced (Fig 6, *F*), as well as mucus production (Fig 6, *G*). In the 1IR model, PG-depleted HDM led to attenuated recruitment of total cells in the BAL, which did not reach significance (Fig E3, *F*) whereas the IgE humoral response was still induced (Fig E3, *G*). T_H2-type cytokines were nonetheless reduced (Fig E3, *H*), as was mucus production (Fig E3, *I*). PG-depleted HDM was also not able to increase airway resistance, as compared to native HDM (Fig E3, *J*). Collectively, these data demonstrate that HDM-induced allergic airway disease depends to a large extent on Nod1 sensing of unique muropeptides derived from the microbiota of the allergen *per se*.

DISCUSSION

In this study, HDM-induced allergic airway disease was strongly decreased in *Nod1*-deficient but not *Nod2*-deficient mice, including BAL cell recruitment, airway resistance, and T_H2-type cytokine expression. Only BAL showed reduced cell recruitment in $Nod2^{-/-}$ compared with WT mice. We presume that this is possibly a consequence of lowered CCL2 levels, as neutralization of this chemokine pathway attenuates macrophage and eosinophil accumulation in the BAL of asthmatic monkeys.[27] HDM challenged $Nod2^{-/-}$ mice were still able to induce lung IL-33 in contrast to $Nod1^{-/-}$ mice, in agreement with the known direct effect of Nod1 on induction of mucosal IL-33 responses.[28] Likewise, similar findings were observed in BEAS-2B cells. One explanation may be that Nod2 ligands are degraded by an amidase activity that is either present in or induced by HDM extracts. Indeed, the presence of a γ-D-glutamyl-L-diamino acid endopeptidase has been described in such extracts.[29] Furthermore, PGLYRP2, an N-acetylmuramoyl-L-alanine amidase, was induced *in vitro* by HDM stimulation in BEAS-2B cells and *in vivo* in the lungs of the HDM model. Alternatively, PEPT2, a transporter mediating the uptake of Nod1 ligands, but not MDP,[30] is thoroughly expressed by the epithelial cells from the respiratory tract,[31] in contrast to PEPT1, a MDP transporter mainly expressed by the gastrointestinal tract.[32] Indeed, PEPT2 mRNA was highly expressed in BEAS-2B cells as well as in the lungs of HDM-challenged mice as compared with PEPT1, likely also explaining the differential activation of Nod1/2 receptors in the lung by HDM. On recognition of PG, both NOD1 and NOD2 undergo self-oligomerization, leading to NF-κB activation and transcription of multiple inflammatory genes on the recruitment of the scaffolding kinase protein RIPK2. In agreement with a recent report[20] and with our data using $Nod1^{-/-}$ mice, $Ripk2^{-/-}$ mice exhibited decreased asthma features in response to HDM, including a decrease in airway resistance. Previous studies have reported conflicting data about the role of Ripk2 in allergic airway inflammation, some finding a promoting effect[20] and others finding none.[33,34] In light of our own data, these results can be reconciled by the presence (or not) of unique muropeptides in the allergen extracts that are used to induce airway inflammation. Consistently, we have previously shown that $Nod1^{-/-}$ mice exhibited similar OVA-induced T_H2-mediated allergic asthma as WT mice did, although a NOD1 agonist used as a systemic adjuvant exacerbated experimental asthma features.[19] It is now well established that alterations in gut microbiota are involved in the susceptibility to asthma.[35] Along this line, Nod1-deficiency has been implicated in intestinal dysbiosis[17] and inhibits the priming of neutrophils by gut-derived PG, resulting in increased susceptibility to pneumococcal lung infection.[36] Even if fecal transplantation experiments excluded the possibility of a pro-allergenic role of the gut microbiota, there is still a possibility in theory that airway microbiota from $Nod1^{-/-}$ mice might contribute to the allergic response in cooperation with the one derived from HDM.

MDP (m/z 494.1990) and its MS/MS fragmentation as described above. The specific fragments are recorded in Table E3. **D,** Dose-dependent effect of HDM on hNOD1, mNod1, and mNod2 reporter activity of HEK293 cells normalized with β-galactosidase. Positive controls: FK565 for hNOD1, FK156 for mNod1, MDP for mNod2. **E,** RE of h*NOD1* and h*NOD2* mRNA in BEAS-2B cells stimulated with HDM. **F,** Inhibitory effect of RIPK2 inhibitor on IL-6 and IL-8 production by HDM- and FK565-stimulated BEAS-2B cells. **G,** Effect of control (*C*) *hNOD1* and *hNOD2* siRNA (*KD*) on HDM-, FK565-, and MDP-induced production of IL-6 by BEAS-2B cells. **H,** HDM-stimulated NHBE cells were examined in terms of dose-dependent cytokine response, of NOD1 and NOD2 RE, and of IL-8 production in the presence of RIPK2 inhibitor. **I,** PGLYRP2 mRNA RE in HDM-stimulated BEAS-2B cells and in lungs from HDM-challenged WT mice. **J,** PEPT1 and PEPT2 mRNA RE in HDM-stimulated BEAS-2B cells and in lungs from HDM-challenged WT mice. Data are presented as mean ± SEM and are representative of 2 to 3 independent *in vitro* experiments and of 10 to 12 mice per group. $^{*}P < .05$, $^{**}P < .01$, $^{***}P < .001$ versus plasmids or medium; $^{\neq}P < .05$, $^{\neq\neq}P < .01$, $^{\neq\neq\neq}P < .001$, 1-way ANOVA **(A-C,F,G),** Kruskal-Wallis test (**D**) and t tests **(E, H** [(NOD1/NOD2], **I, and J)**.

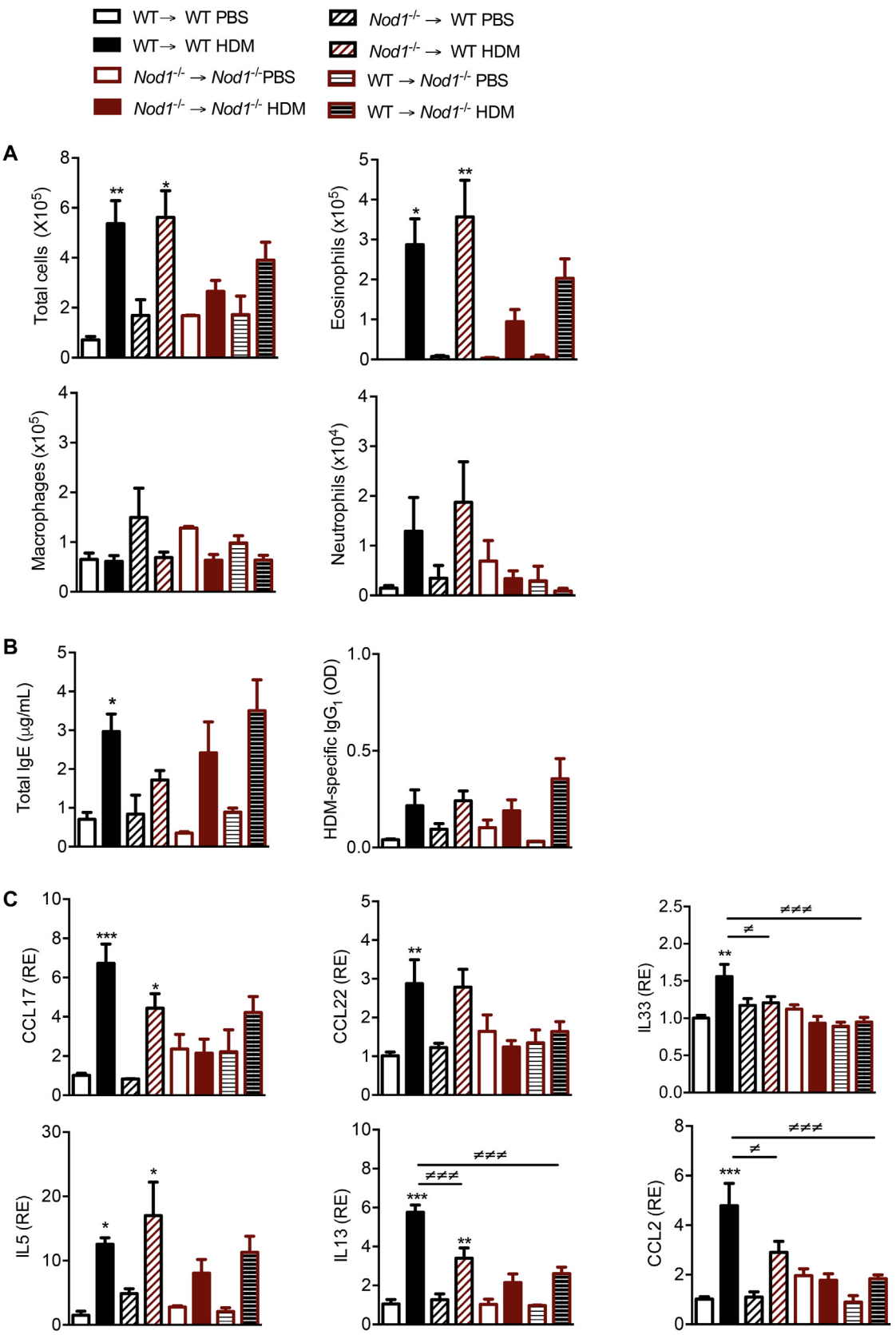

FIG 5. Nod1 expressed by structural cells mediate HDM-induced allergic airway inflammation. Chimeric mice were generated by bone marrow transplantation. **A,** BAL cell counts in WT → WT, *Nod1*$^{-/-}$ → WT (hematopoietic cells deficient in *Nod1*), *Nod1*$^{-/-}$ → *Nod1*$^{-/-}$, and *Nod1*$^{-/-}$ → WT (structural cells deficient in *Nod1*) mice challenged with PBS or high dose of HDM. **B,** ELISA detection of T_H2 humoral response in chimeric mice challenged with PBS or high dose of HDM. **C,** mRNA RE of cytokines and chemokines assessed by quantitative real-time PCR in lung extracts from chimeric mice challenged with PBS or high dose of HDM. Data are presented as mean ± SEM of n = 3 to 6 animals per group. * $P < .05$, ** $P < .01$, *** $P < .001$ versus PBS; $^{\neq}P < .05$, $^{\neq\neq\neq}P < .001$. One-way ANOVA.

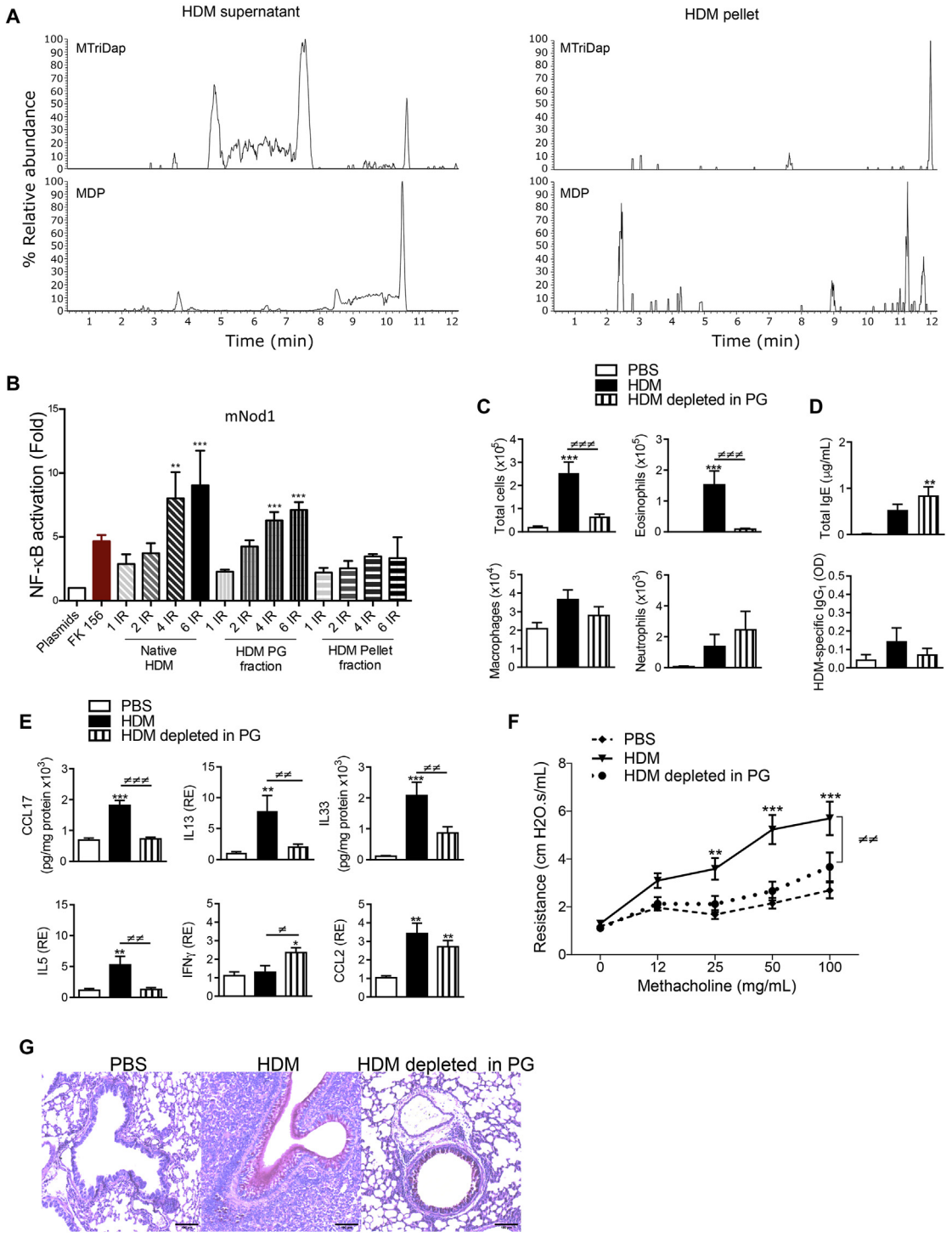

FIG 6. Severity of allergic airway disease is decreased in response to PG-depleted HDM. **A,** Extract ion chromatograms in the PG-containing supernatants and PG-free pellets of HDM extracts after digestion with mutanolysin and precipitation of proteins by organic solvents, corresponding to the protonated MTriDap (m/z 666.2843) and the protonated MDP (m/z 494.1990). **B,** HDM extracts were digested with mutanolysin and proteins precipitated by organic solvents and the activity of the PG-free lysates and the PG-containing supernatants assessed on mNod1 reporter activity. Positive control: FK156. **C,** BAL cell counts in WT mice challenged with PBS or high dose of HDM depleted or not in PG. **D,** ELISA detection of T_H2 humoral response in WT mice challenged with PBS or high dose of HDM depleted or not in PG. **E,** Protein and mRNA expression of cytokines and chemokines assessed by ELISA and quantitative real-time PCR in lung extracts from WT mice challenged with PBS or high dose of HDM depleted or not in PG. **F,** Airway resistance of WT mice challenged with PBS or high dose of HDM depleted or not in PG. **G,** Representative microphotographs of periodic acid–Schiff–stained lung sections in WT mice challenged with PBS or high dose of HDM depleted or not in PG. Bars = 100 μm. Data are presented as mean ± SEM of at least 2 independent *in vitro* experiments, $^{**}P < .01$, $^{***}P < .001$ versus plasmids, and as mean ± SEM of n = 5 to 10 animals per group, $^{*}P < .05$, $^{**}P < .01$, $^{***}P < .001$ versus PBS; $^{\neq}P < .05$, $^{\neq\neq}P < .01$, $^{\neq\neq\neq}P < .001$. One-way ANOVA for all except for airway resistance, which is 2-way ANOVA.

MS analysis of HDM showed the presence of the specific NOD1 ligand DAP-containing muramyl tripeptide, and of the NOD2 ligand MDP. However, in contrast to HDM-induced mNod1 reporter activity, mNod2 reporter activity was only observed in response to 4 times more HDM, suggesting again a putative Nod2 ligand degradation. Although LC-MS analysis confirmed the complete PG depletion, a residual mNod1 reporter activity was observed *in vitro*. This suggests a potential endocytosis of trace PG contaminants that are contained in the animal serum used in the cultures.[37] BEAS-2B cells exhibited a HDM-induced cytokine production that was only partly inhibited by RIPK2 antagonist and by NOD1 siRNA. This partial inhibition may reflect other mechanisms able to induce cytokine production in bronchial epithelial cells in response to other HDM components[38] such as proteases through protease-activated receptor 2 activation[39] or LPSs through TLR4 stimulation.[40] Bone marrow chimeric mice showed that *Nod1*-expressing structural cells were the major cells involved in the aggravated features of HDM-induced airway inflammation which is consistent with the *in vitro* effect observed in epithelial cells. However, the expression of some proinflammatory cytokines was also dependent on hematopoietic cells and probably on dendritic cells that also express NOD1.

It has been proposed that low-dose endotoxin promotes T_H2 responses, whereas high-dose endotoxin promotes T_H1 responses. However, the degree of endotoxin contamination in our extracts was 10 times lower (eg, 10 ng) than the dose used to promote T_H2 immune responses to OVA (eg, 100 ng).[26] Furthermore, LPS-depleted HDM extracts were still able to elicit all the parameters of allergic airway inflammation except for humoral responses, suggesting that LPS, as a major direct stimulus for B cells,[41] is essential in the induction of antibody responses to HDM. This may relate to the predominance of *Bartonella* in HDM extracts, as its LPS has sharply reduced interactions with TLR4.[42] PG depletion from HDM resulted in a similar inhibition than that observed in *Nod1*$^{-/-}$ mice, confirming its role in the exacerbation of HDM-induced allergic airway inflammation. It is of interest that neutralizing antibodies targeting the muropeptide MDP have been recently developed and shown to inhibit PG-dependent autoimmune arthritis.[43] Future development of such PG-neutralizing antibodies would provide further information on the specific role of NOD1 in HDM-induced allergic airway inflammation.

Collectively, this study highlights an unprecedented interaction between NOD1 and HDM, one of the most common allergens, and unveils a new mechanism whereby HDM-derived microbiota is sensed by Nod1 and potentiates disease severity. It paves the way toward novel therapeutic strategies targeting the NOD1 pathway for fighting against the epidemic of asthma.

We thank Stallergenes/Greer for providing *D farinae* extract, and Gabriel Nuñez and Naohiro Inohara (Ann Arbor, Mich) for providing the reporter and expression plasmids for hNOD1, mNod1, and mNod2.

Key messages

- **NOD1-dependent sensing of HDM-associated gram-negative bacteria aggravates experimental asthma.**
- **Inhibition of NOD1 signaling pathway may provide a new therapeutic approach in asthma.**

REFERENCES

1. Goleva E, Jackson LP, Harris JK, Robertson CE, Sutherland ER, Hall CF, et al. The effects of airway microbiome on corticosteroid responsiveness in asthma. Am J Respir Crit Care Med 2013;188:1193-201.
2. Thorsen J, Rasmussen MA, Waage J, Mortensen M, Brejnrod A, Bonnelykke K, et al. Infant airway microbiota and topical immune perturbations in the origins of childhood asthma. Nat Commun 2019;10:5001.
3. Zhou Y, Jackson D, Bacharier LB, Mauger D, Boushey H, Castro M, et al. The upper-airway microbiota and loss of asthma control among asthmatic children. Nat Commun 2019;10:5714.
4. Kim YG, Udayanga KG, Totsuka N, Weinberg JB, Nunez G, Shibuya A. Gut dysbiosis promotes M2 macrophage polarization and allergic airway inflammation via fungi-induced PGE(2). Cell Host Microbe 2014;15:95-102.
5. Li X, Leonardi I, Semon A, Doron I, Gao IH, Putzel GG, et al. Response to fungal dysbiosis by gut-resident CX3CR1(+) mononuclear phagocytes aggravates allergic airway disease. Cell Host Microbe 2018;24:847-56.e4.
6. Chung H, Pamp SJ, Hill JA, Surana NK, Edelman SM, Troy EB, et al. Gut immune maturation depends on colonization with a host-specific microbiota. Cell 2012;149:1578-93.
7. Olszak T, An D, Zeissig S, Vera MP, Richter J, Franke A, et al. Microbial exposure during early life has persistent effects on natural killer T cell function. Science 2012;336:489-93.
8. Russell SL, Gold MJ, Hartmann M, Willing BP, Thorson L, Wlodarska M, et al. Early life antibiotic-driven changes in microbiota enhance susceptibility to allergic asthma. EMBO Rep 2012;13:440-7.
9. Herbst T, Sichelstiel A, Schar C, Yadava K, Burki K, Cahenzli J, et al. Dysregulation of allergic airway inflammation in the absence of microbial colonization. Am J Respir Crit Care Med 2011;184:198-205.
10. Valerio CR, Murray P, Arlian LG, Slater JE. Bacterial 16S ribosomal DNA in house dust mite cultures. J Allergy Clin Immunol 2005;116:1296-300.
11. Lee J, Kim JY, Yi MH, Hwang Y, Lee IY, Nam SH, et al. Comparative microbiome analysis of *Dermatophagoides farinae, Dermatophagoides pteronyssinus,* and *Tyrophagus putrescentiae*. J Allergy Clin Immunol 2019;143:1620-3.
12. Corne JM, Marshall C, Smith S, Schreiber J, Sanderson G, Holgate ST, et al. Frequency, severity, and duration of rhinovirus infections in asthmatic and non-asthmatic individuals: a longitudinal cohort study. Lancet 2002;359:831-4.
13. Ross MA, Curtis L, Scheff PA, Hryhorczuk DO, Ramakrishnan V, Wadden RA, et al. Association of asthma symptoms and severity with indoor bioaerosols. Allergy 2000;55:705-11.
14. Chamaillard M, Hashimoto M, Horie Y, Masumoto J, Qiu S, Saab L, et al. An essential role for NOD1 in host recognition of bacterial peptidoglycan containing diaminopimelic acid. Nat Immunol 2003;4:702-7.
15. Girardin SE, Boneca IG, Carneiro LA, Antignac A, Jehanno M, Viala J, et al. Nod1 detects a unique muropeptide from gram-negative bacterial peptidoglycan. Science 2003;300:1584-7.
16. Girardin SE, Boneca IG, Viala J, Chamaillard M, Labigne A, Thomas G, et al. Nod2 is a general sensor of peptidoglycan through muramyl dipeptide (MDP) detection. J Biol Chem 2003;278:8869-72.
17. Bouskra D, Brezillon C, Berard M, Werts C, Varona R, Boneca IG, et al. Lymphoid tissue genesis induced by commensals through NOD1 regulates intestinal homeostasis. Nature 2008;456:507-10.
18. Hysi P, Kabesch M, Moffatt MF, Schedel M, Carr D, Zhang Y, et al. NOD1 variation, immunoglobulin E and asthma. Hum Mol Genet 2005;14:935-41.
19. Ait Yahia S, Azzaoui I, Everaere L, Vorng H, Chenivesse C, Marquillies P, et al. CCL17 production by dendritic cells is required for NOD1-mediated exacerbation of allergic asthma. Am J Respir Crit Care Med 2014;189:899-908.
20. Miller MH, Shehat MG, Alcedo KP, Spinel LP, Soulakova J, Tigno-Aranjuez JT. Frontline science: RIP2 promotes house dust mite-induced allergic airway inflammation. J Leukoc Biol 2018;104:447-59.
21. Everaere L, Ait-Yahia S, Molendi-Coste O, Vorng H, Quemener S, LeVu P, et al. Innate lymphoid cells contribute to allergic airway disease exacerbation by obesity. J Allergy Clin Immunol 2016;138:1309-18.e11.
22. Kim YG, Park JH, Reimer T, Baker DP, Kawai T, Kumar H, et al. Viral infection augments Nod1/2 signaling to potentiate lethality associated with secondary bacterial infections. Cell Host Microbe 2011;9:496-507.
23. Banskar S, Detzner AA, Juarez-Rodriguez MD, Hozo I, Gupta D, Dziarski R. The Pglyrp1-regulated microbiome enhances experimental allergic asthma. J Immunol 2019;203:3113-25.
24. Park SY, Jing X, Gupta D, Dziarski R. Peptidoglycan recognition protein 1 enhances experimental asthma by promoting Th2 and Th17 and limiting regulatory T cell and plasmacytoid dendritic cell responses. J Immunol 2013;190:3480-92.

25. Yao X, Gao M, Dai C, Meyer KS, Chen J, Keeran KJ, et al. Peptidoglycan recognition protein 1 promotes house dust mite-induced airway inflammation in mice. Am J Respir Cell Mol Biol 2013;49:902-11.
26. Eisenbarth SC, Piggott DA, Huleatt JW, Visintin I, Herrick CA, Bottomly K. Lipopolysaccharide-enhanced, toll-like receptor 4-dependent T helper cell type 2 responses to inhaled antigen. J Exp Med 2002;196:1645-51.
27. Mellado M, Martin de Ana A, Gomez L, Martinez C, Rodriguez-Frade JM. Chemokine receptor 2 blockade prevents asthma in a cynomolgus monkey model. J Pharmacol Exp Ther 2008;324:769-75.
28. Tran LS, Tran D, De Paoli A, D'Costa K, Creed SJ, Ng GZ, et al. NOD1 is required for *Helicobacter pylori* induction of IL-33 responses in gastric epithelial cells. Cell Microbiol 2018;20:e12826.
29. Tang VH, Stewart GA, Chang BJ. House dust mites possess a polymorphic, single domain putative peptidoglycan d,l endopeptidase belonging to the NlpC/P60 Superfamily. FEBS Open Bio 2015;5:813-23.
30. Swaan PW, Bensman T, Bahadduri PM, Hall MW, Sarkar A, Bao S, et al. Bacterial peptide recognition and immune activation facilitated by human peptide transporter PEPT2. Am J Respir Cell Mol Biol 2008;39:536-42.
31. Groneberg DA, Nickolaus M, Springer J, Doring F, Daniel H, Fischer A. Localization of the peptide transporter PEPT2 in the lung: implications for pulmonary oligopeptide uptake. Am J Pathol 2001;158:707-14.
32. Vavricka SR, Musch MW, Chang JE, Nakagawa Y, Phanvijhitsiri K, Waypa TS, et al. hPepT1 transports muramyl dipeptide, activating NF-kappaB and stimulating IL-8 secretion in human colonic Caco2/bbe cells. Gastroenterology 2004;127:1401-9.
33. Kim TH, Park YM, Ryu SW, Kim DJ, Park JH, Park JH. Receptor interacting protein 2 (RIP2) is dispensable for OVA-induced airway inflammation in mice. Allergy Asthma Immunol Res 2014;6:163-8.
34. Nembrini C, Sichelstiel A, Kisielow J, Kurrer M, Kopf M, Marsland BJ. Bacterial-induced protection against allergic inflammation through a multicomponent immunoregulatory mechanism. Thorax 2011;66:755-63.
35. Arrieta MC, Stiemsma LT, Dimitriu PA, Thorson L, Russell S, Yurist-Doutsch S, et al. Early infancy microbial and metabolic alterations affect risk of childhood asthma. Sci Transl Med 2015;7:307ra152.
36. Clarke TB, Davis KM, Lysenko ES, Zhou AY, Yu Y, Weiser JN. Recognition of peptidoglycan from the microbiota by Nod1 enhances systemic innate immunity. Nat Med 2010;16:228-31.
37. Molinaro R, Mukherjee T, Flick R, Philpott DJ, Girardin SE. Trace levels of peptidoglycan in serum underlie the NOD-dependent cytokine response to endoplasmic reticulum stress. J Biol Chem 2019;294:9007-15.
38. Gregory LG, Lloyd CM. Orchestrating house dust mite-associated allergy in the lung. Trends Immunol 2011;32:402-11.
39. Asokananthan N, Graham PT, Stewart DJ, Bakker AJ, Eidne KA, Thompson PJ, et al. House dust mite allergens induce proinflammatory cytokines from respiratory epithelial cells: the cysteine protease allergen, Der p 1, activates protease-activated receptor (PAR)-2 and inactivates PAR-1. J Immunol 2002;169:4572-8.
40. Hammad H, Chieppa M, Perros F, Willart MA, Germain RN, Lambrecht BN. House dust mite allergen induces asthma via Toll-like receptor 4 triggering of airway structural cells. Nat Med 2009;15:410-6.
41. Lu M, Munford R. LPS stimulates IgM production in vivo without help from non-B cells. Innate Immun 2016;22:307-15.
42. Zahringer U, Lindner B, Knirel YA, van den Akker WM, Hiestand R, Heine H, et al. Structure and biological activity of the short-chain lipopolysaccharide from *Bartonella henselae* ATCC 49882T. J Biol Chem 2004;279:21046-54.
43. Huang Z, Wang J, Xu X, Wang H, Qiao Y, Chu WC, et al. Antibody neutralization of microbiota-derived circulating peptidoglycan dampens inflammation and ameliorates autoimmunity. Nat Microbiol 2019;4:766-73.